Application of CRS technique to poor quality of seismic signal data

The present study demonstrates the application of Common-Reflection-Surface (CRS) technology to vintage seismic data acquired in the North-West territory of Uzbekistan. Application of this technology enabled achieving proper data regularization as well as an enhancement in the signal-to-noise ratio.

Introduction

Conducting field seismic surveying operations according to a regularly designed system almost always encounters difficulties in placing sources and receivers in various exclusive zones, resulting in irregularity in acquired data. There are methods for data regularization, such as triangulation or Fourier transformation (3D, 5D regularization). However, these technologies operate on data within the framework of the CMP concept, implying reflection from an absolutely horizontal surface. This can lead to both explicit artefacts (phase-to-phase transition) and hidden ones (distortion of signal dynamic characteristics) in the case of large angles of inclination of reflecting surfaces. CRS allows obtaining regular data while preserving the signal's dynamic characteristics and enhancing the signal-to-noise ratio. The CRS method was developed by Professor Hubral and represents an evolution of the ideas of constructing sections in the time domain by Gelchinsky and Bazelaire (Hubral, 1983; de Bazelaire, 1988; Gelchinsky, 1988).

Method

Within the framework of CRS summation, the medium is considered as a model with curved interfaces characterized by their arrangement, local curvature, and local dip direction. For seismic data recorded on the surface with multiple overlaps, the wave is characterized by the exit angle and two radii of curvature of the wave field:

α — the exit angle of the ray normal to the depth reflecting horizon at the surface,

R_{NIP} — the radius of curvature of the wave for a point source located at the point of normal incidence (NIP).

R_N — the radius of curvature of the wave obtained during modelling of the "radiating" horizon.

These three parameters of the wave field determine the summation surface for seismic data with multiple overlaps, which is not limited by CMP geometry. A well-described detail of the CRS technology is provided in the work of Jaeger et al. (Jaeger et al., 2001).

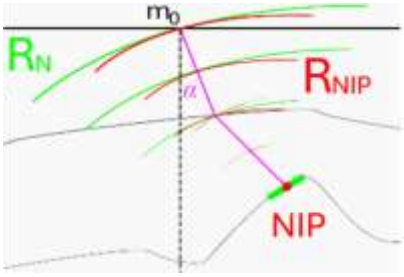

Figure 1. CRS attributes.

Data description

The seismic data obtained for reprocessing consisted of 2D and 3D data and different surveys. These data were acquired at different times (from 1994 to 2010), using various types of sources (vibratory and explosive) and different recording parameters. It is also necessary to note the low fold coverage due to the low channel count (48 channels for most 2D data). The 3D data is also quite sparse: the inline and crossline for 3D spacing are 50m and 600m, respectively, resulting in a CDP grid of 25x25 m with a nominal fold of 24. The sweep is 10-90 Hz and 12 seconds in length.

Before implementing CRS technology, data underwent gain and amplitude balancing in both the source and receiver domains to address significant differences in source gains, which led to signal penetration issues. Noise bursts and noisy data filtering were performed in both the shot and receiver domains using a novel amplitude thresholding technique developed specifically for this project, outperforming the standard time-frequency-denoise (TFD) process in terms of both speed and quality. However, obtaining velocity functions on CMP gathers was challenging even after denoising, especially in the deep sections where no signals were visible (Figure 2, left). During the process, the CRS algorithm requires an initial RMS velocity function for NMO purposes. A perfect function is not critical for the CRS process. After applying the CRS process, estimating the velocity function became much easier (Figure 2, right). Figure 2 shows examples of velocity analysis at one of the CMP gathers and its semblance before and after CRS application.

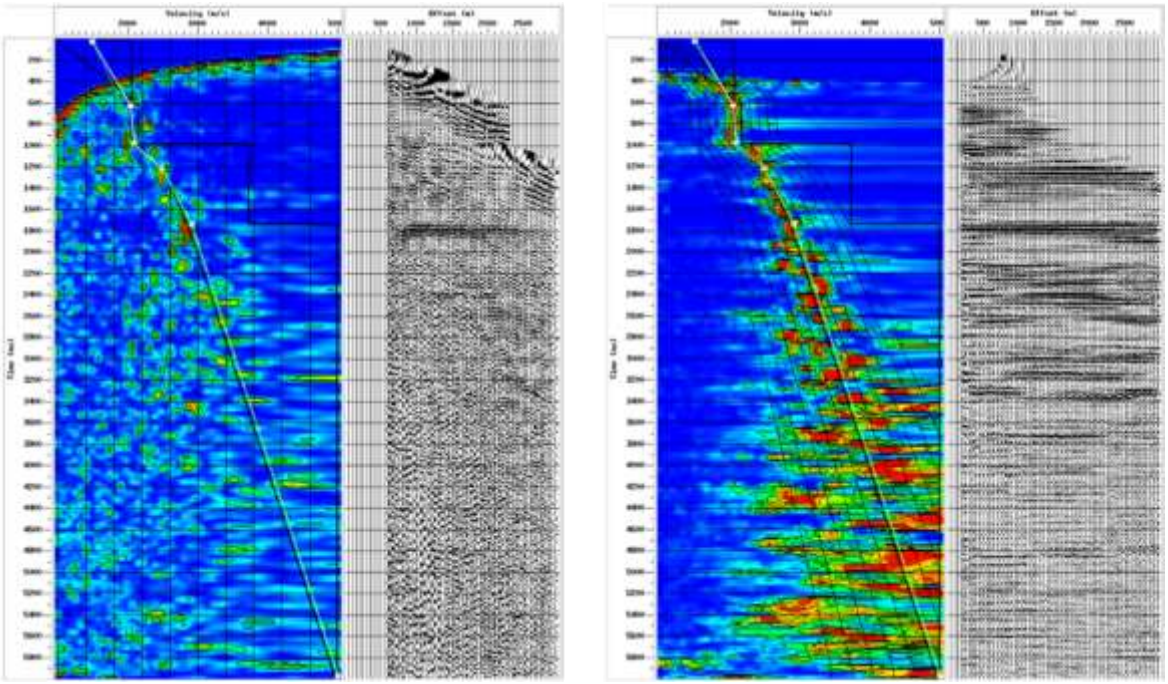

Figure 2. CMP time gathers and semblance with vertical velocity functions before (left) and after (right) CRS.

Figure 3 shows CMP gathers before CRS (left) and after (right). The reflectors are clearly visible and continuous.

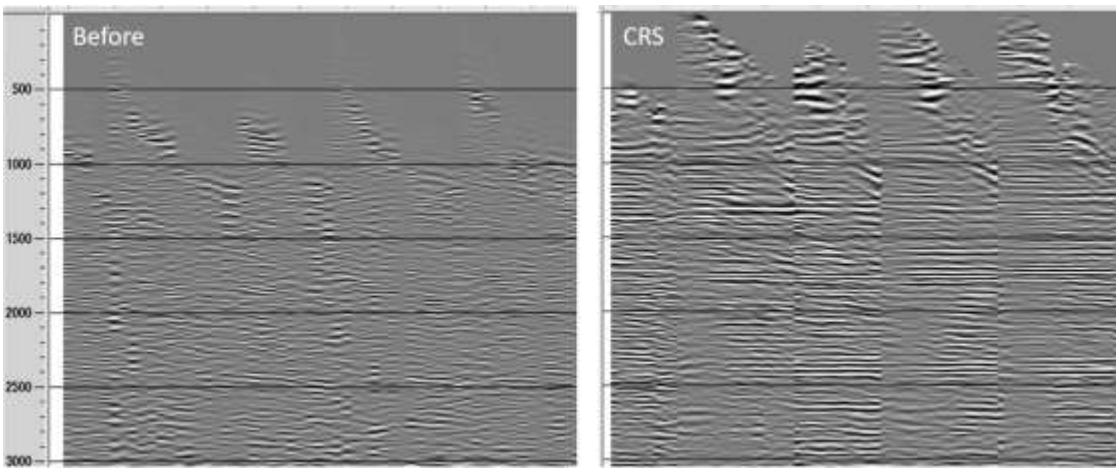

Figure 3. CMP time gathers before CRS (left) and after (right).

Figures 4 and 5 show zoom to shallow and deep parts of 3D seismic sections before and after CRS. After using CRS, we see improvements throughout the section, especially in tracing dipping reflections between 3500-4500. It is easy to notice that CRS stack has better continuous reflectors that benefit structural interpretation. This enhancement is undoubtedly due to CRS offering a clearer depiction of reflected wavefronts, outperforming traditional seismic methods.

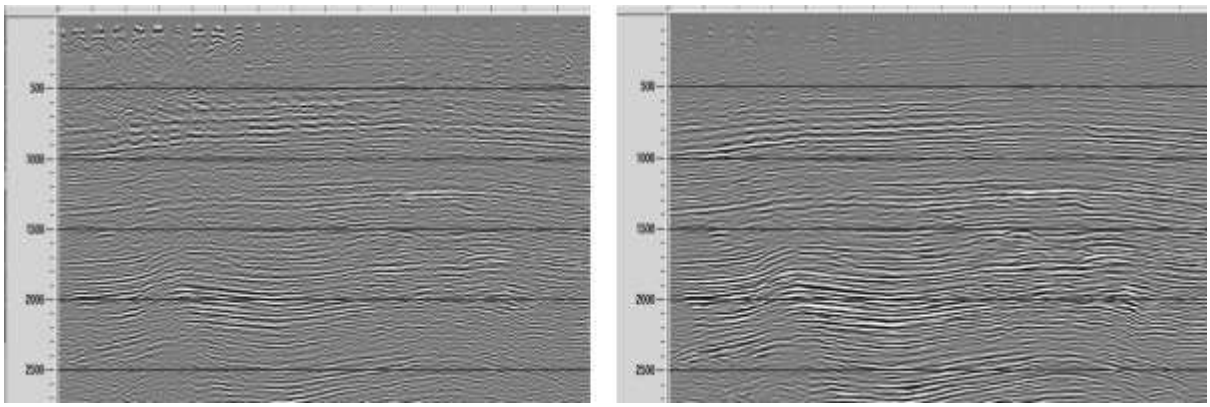

Figure 4. Shallow part, seismic time sections before CRS (left) and after (right).

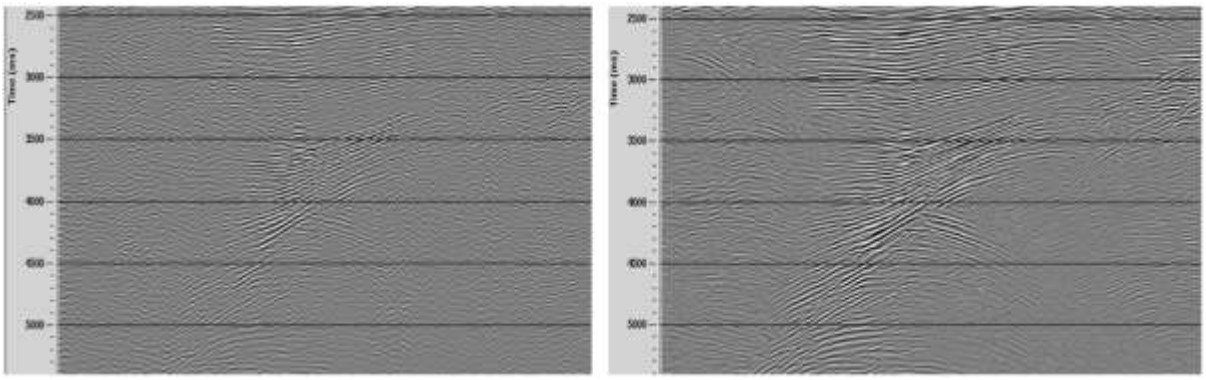

Figure 5. Deep part seismic time sections before CRS (left) and after (right).

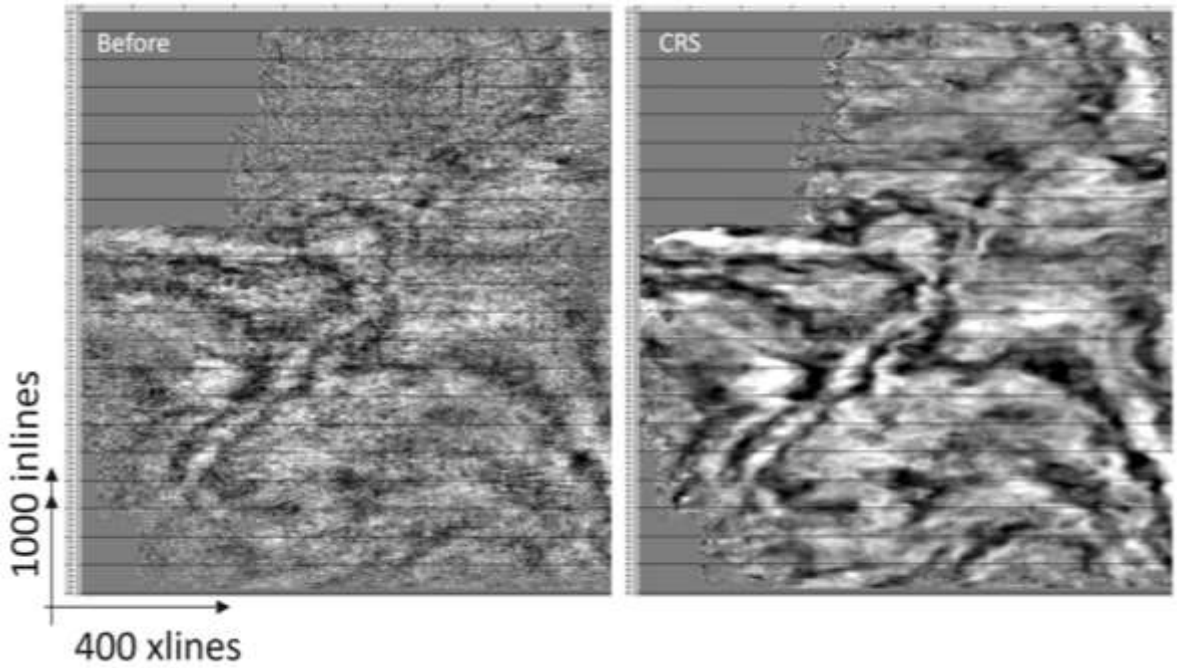

Figure 6. Time slices before CRS (left) and after (right).

Figure 6 shows time slices of parts of the 3D cubes before and after CRS. The significant improvement in signal-to-noise ratio and reduction of the footprint effect are clearly evident. Despite the sparsity of acquired data, more geological features are now discernible. Notably, structures in the northern region were indistinguishable before applying the CRS technique. It should be emphasized that the seismic data shown in the illustrations has not undergone migration. Figure 7 shows migrated non-CRS data and CRS data without post-migration processes applied for both cases. It is easy to notice that a fault complex on the left side of the right section is one of the main achievements the reprocessing was aimed for.

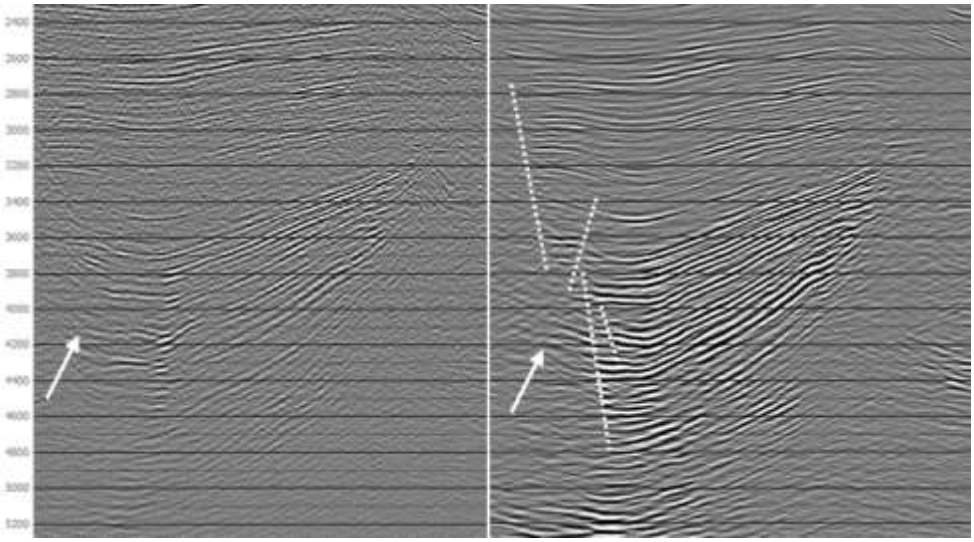

Figure 6. Pre-stack Kirchhoff time migrated time sections, no CRS (left) and with CRS (right).

Conclusion

The application of CRS technology has enabled an increase in the signal-to-noise ratio, accelerated the analysis of velocities, and improved the accuracy of their determination. Additionally, proper data regularization has been achieved, allowing for more accurate mapping of faults and structural traps, as well as obtaining dynamic characteristics correlating with well data. While various approaches were tested for these vintage data, CRS was the main factor for success.

Acknowledgements

The author acknowledges and appreciates Yangi Kon Ltd, Uzbekistan, for granting permission to showcase our results.

References

1. de Bazelaire, E. [1988] Normal-moveout correction revisited: Inhomogeneous media and curved interfaces: Geophysics, 53, 143–157.
2. Gelchinsky, B., [1988], The common-reflecting-element (CRE) method: ASEG/SEG Internat. Geophys. Conf., Extended Abstracts, 71–75.
3. Hocht G., de Bazelaire E., Majer P., Hubral P. [1999] Seismic and optics: hyperbolae and curvatures: J. Appl. Geoph., 42 (3, 4), 261-281.
4. Hubral P., [1983] Computing true amplitude reflections in a laterally inhomogeneous ears: Geophysics, 48, 8, 1051-1062.
5. Jager R., Mann J., Hocht G., Hubral P. [2001] Common-reflection-surface stack: image and attributes: Geophysics, 66, 1, 97-109.